J. Braz. Chem. Soc., Vol. 19, No. 6, 1224-1229, 2008.
Printed in Brazil - ©2008 Sociedade Brasileira de Química
0103 - 5053 $6.00+0.00

Article

Synthesis of Ag-PVA and Ag-PVA/PET-s20 Composites by Supercritical CO_2 Method and Study of Silver Nanoparticle Growth

Rafael Silva, Marcos H. Kunita, Emerson M. Girotto, Eduardo Radovanovic, Edvani C. Muniz, Gizilene M. Carvalho and Adley F. Rubira*

Grupo de Materiais Poliméricos e Compósitos, Departamento de Química, Universidade Estadual de Maringá, Av. Colombo 5790, 87020-900 Maringá-PR, Brazil

CO_2 supercrítico foi utilizado para preparar compósitos poliméricos com prata, prata/poli álcool vinílico e prata/ poli álcool vinílico/ poli (tereftalato de etileno) sulfonado, pela impregnação de um precursor de prata nas matrizes poliméricas no estado sólido seguida da redução térmica do precursor. Difração de raio X, microscopia eletrônica de varredura, espectroscopia de energia dispersiva, microscopia de força atômica, análise termogravimétrica e espectroscopia no UV/vis dos compósitos indicaram que as condições de preparação e a composição da matriz polimérica influenciam o tamanho e a forma das partículas de prata formadas, assim como, a uniformidade e a distribuição das partículas nas matrizes poliméricas. As partículas de prata nos compósitos ricos em PVA são menores, possuem formas mais uniformes e apresentam distribuição de tamanho mais estreita do que nos compósitos ricos em PETs.

Supercritical CO_2 has been used to prepare silver polymer composites, silver/poly(vinyl alcohol) and silver/poly(vinyl alcohol)/sulfonated poly(ethylene terephthalate) through impregnation of a silver precursor in solid-state polymeric matrices followed by thermal reduction of the silver precursor. X-ray diffraction, scanning electron microscopy, energy dispersive spectroscopy, atomic force microscopy, thermogravimetric analysis and UV/vis spectroscopy indicate that synthesis conditions and polymeric matrix composition affect silver particle size, shape and distribution in polymeric matrices. Silver particles are smaller, have a more uniform shape and present narrower size distribution in PVA-rich than in PETs-rich composites.

Keywords: composites, polymers, surfaces, crystal growth, electron microscopy

Introduction

Nanostructured silver particles in zero oxidation state have been object of great interest for decades due to their use in catalysis, photography, photonics, electronics, information storage, labeling, imaging, sensing, and surface-enhanced Raman scattering (SERS).[1-6] In the several works with different preparation methods reported, the silver precursor, a silver salt, is reduced in solution in the presence of a capping agent.[7-14] The polyol process has been known for decades as a generic route for the synthesis of metal colloids.[12-14] It concerns the preparation of metallic powders, essentially of cobalt, nickel, copper, and precious metals, by reduction of inorganic compounds in liquid polyol, which acts both as a solvent and a reducing agent, as stated by Blin *et al.*[15] In recent works on the polyol reaction mechanism, Shengming *et al.*[16,17] showed that polyol is oxidized during the process and produces CO_2 molecules, which are detected as carbonate ions.

Recently, supercritical fluids have been applied to obtaining new materials.[18] Supercritical state has been studied and reported in literature since its discovery in the early 19th century by Baron La Tour.[19] Supercritical fluids allow controlling particle shape and size to produce highly uniform nanometric materials. Silver nanoparticles, nanobanners, and nanowires were obtained by reduction of Ag_2O in supercritical water by Chang *et al.*[20] Reverchon and Adami[21] compared several synthesis and stabilization methods of noble metal nanoparticles with supercritical CO_2. The use of supercritical fluids offers the benefit of high diffusivity besides its ecological advantages, and particularly the solvation power of supercritical CO_2, which may be used as a swelling agent, as reported by Kunita *et al.*[23]

*e-mail: afrubira@uem.br

The present work reports on the production of silver nanoparticles embedded in a solid-state poly(vinyl alcohol) (PVA) host and in its blends with sulfonated poly(ethylene terephthalate) (PET-s20) through impregnation process using supercritical CO_2 and a silver precursor. Due to the high diffusivity of supercritical CO_2, the whole solid-state polymeric bulk becomes accessible to the silver precursor, which is dissolved in supercritical CO_2. The goals of this work are to evaluate a synthesis method of silver nanoparticles in a solid-state host matrix and investigate the influence of synthesis parameters and matrix characteristic on the distribution, shape, and size of silver particles.

The composites were characterized by X-ray diffraction (XRD), scanning electron microscopy (SEM), energy dispersive spectroscopy (EDS), atomic force microscopy (AFM), UV/vis spectroscopy, and thermogravimetric analysis (TGA).

Experimental

Materials and apparatus

Water soluble sulfonated PET ionomer, PET-s20 (20% sulfonated), trade name Gerol® PS-20, was provided by Rhodia (structure shown in Figure 01). PVA, poly (vinyl alcohol), (13.000-26.000 u), 98% hydrolyzed, and the silver precursor 1,5-cyclooctadiene-1,1,1,5,5,5-hexafluoroacetylacetonate silver (I) dimer ([Ag(COD) HFEA]$_2$, and CO_2 were purchased from Aldrich and White Martins, respectively.

X-ray diffractograms were obtained on D-6000 Shimadzu, using Cu Kα radiation (λ = 1.5406 Å), operating at room temperature. The data were collected in the range from 10 to 90° 2θ, the scanning parameters were set at 0.02° 2θ step width, count time 0.6 s. SEM was performed on SHIMADZU SS-550. A Shimadzu SPM-9500J3 atomic force microscope (AFM) was used to analyze surface morphology. EDS was carried out on Noran System Six coupled to a Jeol JSM 6360 LV SEM. Thermogravimetric analyses were conducted on SHIMADZU TGA-50, with nitrogen flow rate of 20 mL min^{-1} and heating rate of 10 ºC min^{-1}.

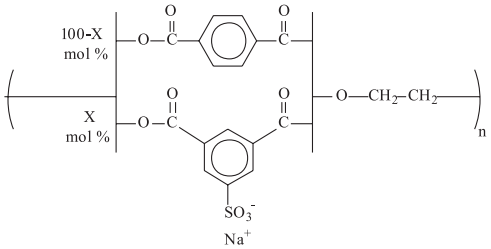

Figure 1. Molecular structure of PET-s20, X=20.

Polymeric films

PVA, PET-s20, and PVA/PET-s20 polymeric blend films (mass ratios of 20/80, 40/60, 60/40, and 80/20) were cast with Millipore water as a solvent at room temperature (25 ºC).

Infusion of silver complex into PVA and PVA/PET-s20 blends using supercritical CO_2

The infusion process was carried out with carbon dioxide (White Martins) 99.95% pure on Thar, model SFE 500. The infusion vessel (*ca*. 25 mL) was charged with the silver precursor and the polymeric film in a 20% mass proportion of silver. The silver complex was placed in a silica porous support to avoid its physical contact with the polymeric film. The vessel was purged with CO_2 and closed. After the system had reached thermal equilibrium, CO_2 was pumped in until the desired pressure was reached. The impregnation conditions of the polymeric films with the silver precursor are shown in Table 1.

Table 1. Impregnation conditions

Conditions	time/(h)	Pressure/(atm)	Temperature /(ºC)
a	5	120	60
b	4	150	80

Thermal treatments

The silver precursor-impregnated films were thermally treated in an oven with ambient air circulation in different controlled temperature and time conditions.

Results and Discussion

The thermal treatment of the silver complex-infused PVA film resulted in the reduction of silver to zero oxidation state, as evidenced by the X-ray diffractogram in Figure 2. Ag-PVA composites present interesting spectral characteristics depending on the impregnation and thermal treatment conditions. In the thermal treatment, the composite, which is initially light brown due the presence of the silver complex, becomes a yellow transparent film in a few minutes. After some minutes of thermal treatment, a reflective mirror surface is observed. The formation of the reflective mirror occurs due the agglomeration of silver particles on the surface. The polymer chain mobility increases during the thermal treatment; consequently, the silver particles also have mobility in the composite bulk phase and the silver particles agglomerate, since their movement toward the surface is irreversible.

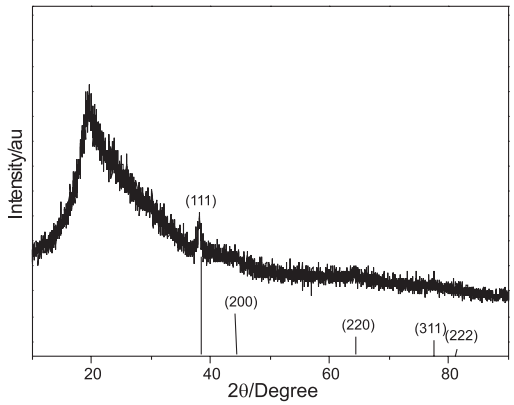

Figure 2. X-ray diffractogram of Ag-PVA composite thermally treated at 100 ºC for 15 min.

Under the same thermal treatment conditions and impregnation condition *a* (Figure 3a), the composite films obtained presented a more intense metallic shine than under impregnation condition *b* (Figure 3b). The more intense metallic shine of condition *a* films is due to their more uniform particle shape, distribution, and size when compared to those of condition *b* films. The formation of silver aggregates on condition *b* films must be assigned to the heterogeneous distribution of the silver precursor in the polymeric matrix obtained during the impregnation process. The increase in time, temperature, and pressure values favors the reduction of the silver precursor in the polymer matrix directly, as also found by others authors.[23-26] The reduction of the silver precursor during the impregnation process hinders the dispersion of silver due to the insolubility of metallic silver in supercritical CO_2. Consequently, the agglomeration of silver particles during the thermal treatment is provided by the heterogeneous distribution of silver in the polymeric matrix. Since the aim of the impregnation process is to disperse the silver precursor in the polymeric matrix, condition *a* is more appropriate to this end comparatively to condition *b*.

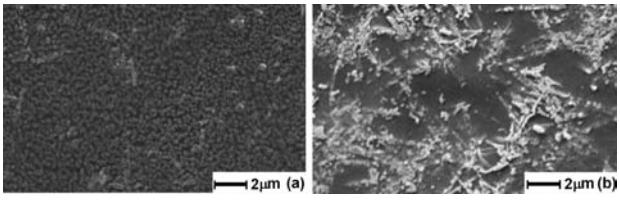

Figure 3. Surface SEM micrographs of Ag-PVA composites impregnated under conditions *a* (a) and *b* (b), and thermally treated under similar conditions, t = 30 min, T = 135 ºC.

The morphology of Ag-PVA composites is highly dependent on thermal treatment conditions. Impregnation in condition ***a*** was used in the study of the thermal treatment influence. Figure 4 shows the micrographs of Ag-PVA composites obtained under different thermal treatment conditions ((a) t = 60 min, T = 90 ºC; (b) t = 30 min, T = 135 ºC; (c) t = 90 min, T = 135 ºC; and (d) t = 300 min, T = 150 ºC). While the silver precursor decomposes (reduction to Ag) during the thermal treatment, the metallic silver particles grow (Figure 4). The first particles formed may have a diameter of only a few nanometers, if one considers Ostwald ripening in this system.[27] The small silver particles at the beginning of the thermal treatment tend to agglomerate after some time. This spontaneous process occurs because the chemical potential of the small particles is higher than that of the large ones due to the ratio between the silver crystal internal and surface atoms, which increases abruptly as the particle diameter decreases. Under long high temperature thermal treatment, Figure 4d, needle-like silver structures are formed due to the longitudinal particle coalescence.

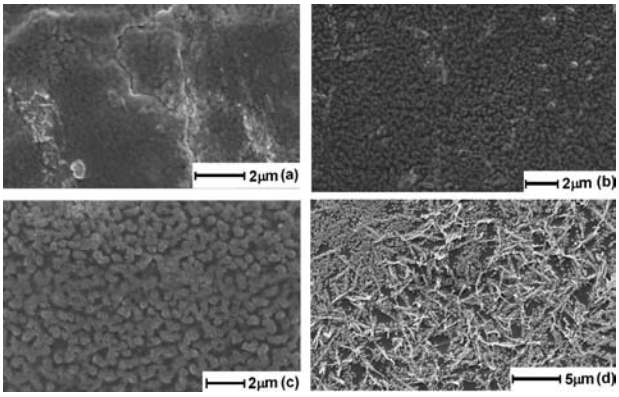

Figure 4. SEM micrographs of silver-impregnated PVA thermally treated under different conditions. (a) t = 60 min, T = 90 ºC; (b) t = 30 min, T = 135 ºC; (c) t = 90 min, T = 135 ºC; (d) t = 300 min, T = 150 ºC.

The AFM image of composite Ag-PVA obtained under thermal treatment conditions T = 135 ºC and t = 30 min, Figure 5, indicates the presence of spherical particles with mean diameter of 80 nm on the film surface.

In the polyol process, the polyol hydroxyl groups are responsible for the reduction and stabilization of the silver nanoparticles in solution.[12-14] PVA and PETs blends with different compositions were used to evaluate the influence of the polymer matrix on the formation of the silver nanoparticles in solid state. Figure 6 shows that the morphology of the Ag-PVA/PET-s20 composite treated at 135 ºC for 30 min is directly related to the blend composition and that blends with high PETs content are less uniform. Silver particles agglomerate in composites Ag-PVA/PET-s20 20/80 and Ag-PVA/PET-s20 40/60, whereas for composites Ag-PVA/PET-s20 60/40 and Ag-PVA/PET-s20 80/20, they are distributed all over the surface. Among the Ag-PVA/PET-s20 composites, composite 60/40 has the smallest silver particles, which are

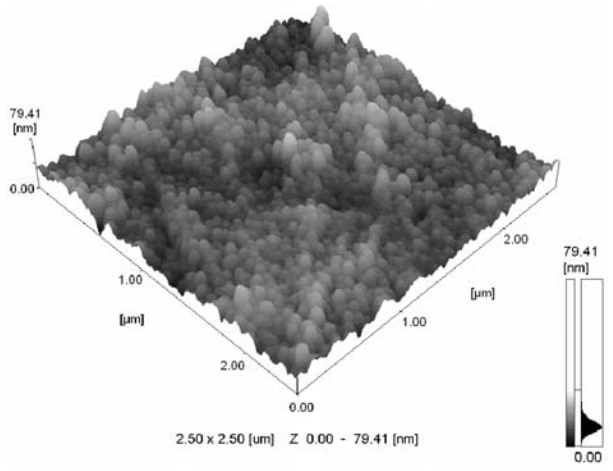

Figure 5. AFM image of silver-impregnated PVA thermally treated at 135 ºC for 30 min.

larger than 200 nm. The composite AFM image is shown in Figure 7. The AFM images of composites Ag-PVA and Ag-PVA/PET-s20 60/40 (Figure 5 and Figure 7, respectively) indicate that the addition of PET-s20 leads to an increase in silver particle size.

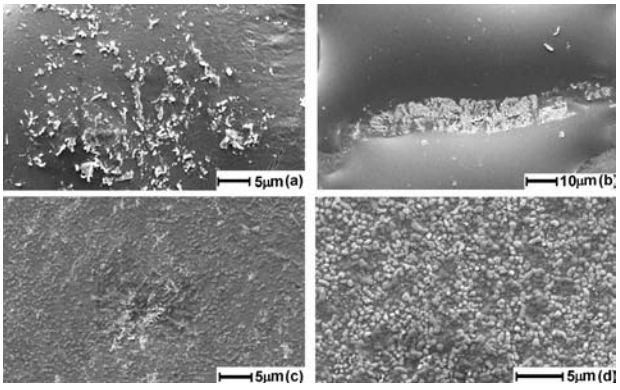

Figure 6. SEM micrographs of silver-impregnated PVA/PET-s20 blends thermally treated at 135 ºC for 30 min. (a) PVA/PET-s20 20/80, (b) PVA/PET-s20 40/60, (c) PVA/PET-s20 60/40, and (d) PVA/PET-s20 80/20.

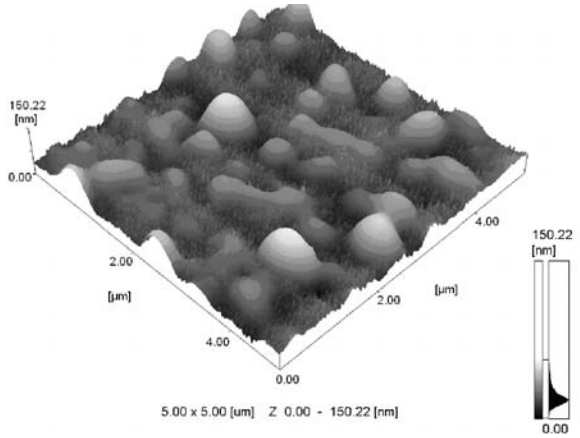

Figure 7. AFM image of PVA/PET-s20 60/40 (wt.%/wt.%) composite thermally treated at 135 ºC for 30 min.

The study of the composite surface layer chemical composition by EDS enabled us to relate the amount of silver in the surface layers to the PET-s20 blend content. Figure 8 shows that the amount of silver on the surface layers increases exponentially as the PET-s20 content in the polymeric matrix increases. The increase in silver particle size by the addition of PETs to the polymeric matrix verified by SEM and AFM is directly correlated with the high concentration of silver on the surface of PETs-rich blends. The agglomeration of silver on the surface of PETs-rich blend is caused by the heterogeneous distribution of the silver complex, which, in turn, may be due to small affinity of the silver complex for the polymer matrix comparatively to that of PVA-rich blends.

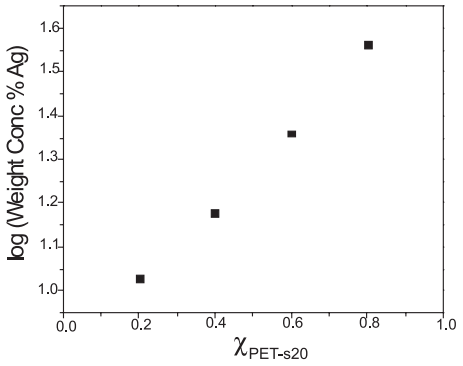

Figure 8. Silver weight concentration on composite surface as a function of PET-s20 weight fraction (χ) in blends.

The collective oscillation of conduction electrons in Ag nanostructures results in surface plasmon resonance (SPR). As confirmed by various studies, the SPR properties of metal nanostructures are strongly dependent on parameters such as size, shape, composition, crystallinity, and structure.[23] The UV/Vis absorption spectra of the composites shown in Figure 9 may be used to study the nucleation process, since the UV/Vis absorption spectra were obtained for thermally treated samples without the reflective mirror (yellow transparent films). The spectra exhibit the characteristic surface plasmon absorption band of nanoscale Ag particles at around 400 nm. Figure 9 shows that Ag-PVA and Ag-PVA/PET-s20 80/20 composites present the surface plasmon absorption band at a lower wavelength and a bandwidth narrower than that of the nanoparticles in the other composites. Therefore, the silver nanoparticles are smaller and have narrower size distribution in Ag-PVA and Ag-PVA/PET-s20 80/20 than in PETs-rich composites.

In addition, PETs-rich composite spectra (Figure 9, spectra c and d) present a shoulder at around 512 nm, indicating the presence of non-spherical silver particles. Silver

nanoparticles with different shapes, such as hollow spheres, anisotropic cubes, and octahedral, are responsible for the SPR bands in this region, as reported by Wiley *et al*.[28]

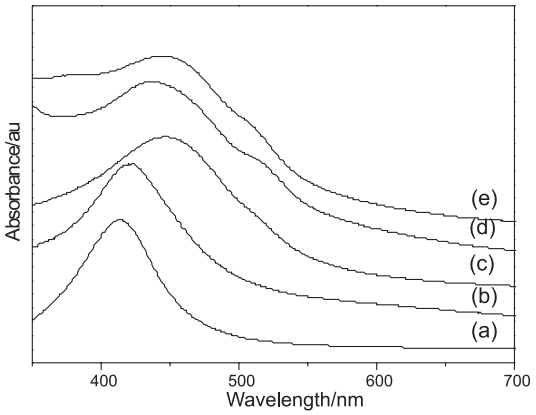

Figure 9. Absorption spectra of silver composites thermally treated at 100 ºC for 15 min. (a) Ag-PVA, (b) Ag-PVA/PET-s20 80/20, (c) Ag-PVA/PET-s20 60/40, (d) PVA/PET-s20 40/60, and (e) PVA/PET-s20 20/80

The changes in silver particle size and size distribution caused by the addition of PETs to the polymeric matrix provide evidence that the formation of silver particles in solid hosts, as well as in solutions, may be favored by the presence of hydroxyl groups. The presence of small particles in PVA-rich composites may be understood in terms of the action of hydroxyl groups as a reducing agent that also stabilizes the silver nanoparticles as a capping agent.

The thermal stability of the pure polymer, the blends, and the composites was evaluated by thermogravimetric analysis (TGA). Table 2 shows polymer decomposition temperature data of the samples analyzed at 10%-level mass loss temperatures (PDT_{10}). The composite thermal stability is lower than those of the polymers and blends are, indicating that silver acts as a pyrolysis catalyst. This agrees with pyrolysis data of similar systems with similar behaviors.[25]

Table 2. Pure polymer blend and composite decomposition temperature as a function of 10% mass loss (PDT_{10})

Polymeric Matrix	PDT_{10} of pure polymer and blends/(ºC)	PDT_{10} of composites/(ºC)
PVA	293	277
PET-s20	390	300
PVA/PET-s20 20/80	341	254
PVA/PET-s20 40/60	308	270
PVA/PET-s20 60/40	292	252
PVA/PET-s20 80/20	298	269

Conclusion

Supercritical impregnation condition ***a*** (pressure = 120 atm, temperature = 60 ºC, impregnation = 5 h) proved to be appropriate for obtaining Ag-PVA and Ag-PVA/PET-s20 composites.

The amount of silver on the composite surface increases exponentially as the blend PET-s20 content increases. The morphology of composite Ag-PVA/PET-s20 is highly dependent on blend composition. Silver aggregates on the surface of composites with high PET-s20 contents, which suggests that silver disperses more effectively through composite polymeric matrices with high PVA contents.

The process presented here may be applied to prepare silver nanoparticles in a polymeric support with controlled particle size and shape by varying treatment temperature and time.

Silver nanoparticles in PVA-rich composites are smaller, have more uniform shape, and present narrower size distribution than those in PETs-rich composites, indicating the probable reducing action of PVA hydroxyl groups on silver.

Acknowledgments

The authors thank CNPq and Fundação Araucária (foundation that supports technologic and scientific development in the State of Paraná, Brazil) for the financial support.

References

1. Jin, R.; Cao, Y. W.; Mirkin, A.; Kelly, K. L.; Schatz, G. C.; Zhang, J. G.; *Science.* **2001,** *294,* 1901.
2. Wang, H.; Qiao, X.; Chen, J.; Wang, X.; Ding, S.; *Mater. Chem. Phys.* **2005**, *94*, 449.
3. Zhang, X.; Young, M. A.; Lyandres, O.; Van Duyne, R. P.; *J. Am. Chem. Soc.* **2005**, *127*, 4484.
4. Chen, J.; Saeki, F.; Wiley, B. J.; Cang, H.; Cobb, M. J.; Li, Z.-Y.; Au, L.; Zhang, H.; Kimmey, M. B.; Li, X.; Xia, Y.; *Nano Lett.* **2005**, *5*, 473.
5. Porel, S.; Singh, S.; Harsha, S. S.; Rao, D. N.; Radhakrishnan, T. P.; *Chem. Mater.* **2005**, *17*, 9.
6. Rao, C. R. K., Trevedi, D. C.; *Mater. Chem. Phys.* **2006,** *99,* 354.
7. Zhang, D.; Qi, L.; Ma, J.; Cheng, H.; *Chem. Mater.* **2001,** *13,* 2753.
8. Naik, R. R.; Stringer, S. J.; Agarwal, G.; Jones, S. E.; Stone, M. O.; *Nat. Mater.* **2002,** *1,* 169.
9. Temgire, M. K.; Joshi, S. S.; *Radiat. Phys. Chem.* **2004,** *71,* 1039.

10. Khanna, P. K.; Singh, N.; Charan, S.; Subbarao, V. V. V. S.; Gokhale, R.; Mulik, U. P.; *Mater. Chem. Phys.* **2005,** *93*, 117.
11. Oliveira, M. M.; Castro, E. G.; Canestraro, C. D.; Zanchet, D.; Ugarte, D.; Roman, L. S.; Zarbin, A. J. G.; *J. Phys. Chem. B* **2006,** *110*, 17063.
12. Kim, D. W.; Lee, J. M.; Lee, J. J.; Kang, P. Y.; Kim, Y. C.; Oh, S. G.; *Surf. Coat. Technol.* **2007,** *201*, 7663.
13. Chen, C.; Wang, L.; Yu, H.; Wang, J.; Zhou, J.; Tan, I.; Deng, L.; *Nanotechnology* **2007,** *18*, 115612.
14. Gautam, A.; Singh, G. P.; Ram, S.; *Synth. Met.* **2007,** *157*, 5.
15. Blin, B.; Fiévet, F.; Beaupere, D.; Figlarz, M.; *New J. Chem.* **1989**, *13*, 67.
16. Ying, Z.; Shengming, J.; Guanzhou, Q.; Min, Y.: *Mater. Sci. Eng. B* **2005,** *122*, 222.
17. Shengming, J.; Liangsheng, Y.; Ying, Z.; Guanzhou, Q.; Cuifeng, W.; *Mater. Res. Bull.* **2006,** *41*, 2130.
18. Hakuta, Y.; Haganuma, T.; Sue, K.; Adschiri, T.; Arai, K.; *Mater. Res. Bull.* **2003,** *38*, 1257.
19. Tour, C. C.; *Ann. Chim. Phys.* **1822,** *21*, 127.
20. Chang, J. Y.; Chang, J. J.; Lo, B.; Tzing, S. H.; Ling, Y. C.; *Chem. Phys. Lett.* **2003**, *379*, 261.
21. Reverchon, E.; Adami, R.; *J. Supercrit. Fluids.* **2006,** *37*, 1.
22. Kunita, M. H.; Rinaldi, A. W.; Girotto, E. M.; Radovanovic, E.; Muniz, E. C.; Rubira, A. F.; *Eur. Polym. J.* **2005**, *41*, 2176.
23. Silvert, P-Y.; Urbina, R. H.; Duvauchelle, N.; Vijayakrishnan V.; Elhsissen, K. T.; *J. Mater. Chem.* **1996,** *6*, 573.
24. Silvert, P-Y.; Urbina, R. H.; Elhsissen, K. T.; *J. Mater. Chem.* **1997,** *7*, 293.
25. Nazem, N.; Taylor, L. T.; Rubira, A. F.; *J. Supercrit. Fluids* **2002,** *23*, 43.
26. Otsu, J.; Oshima, Y.; *J. Supercrit. Fluids* **2005**, *33*, 61.
27. Petersen, M.; Zangwill, A.; Ratsch, C.; *Surf. Sci.* **2003,** *536*, 55.
28. Wiley, B. J.; Im, S. H.; Li, Z.Y.; Mclellan, J.; Siekkinen, A.; Xia, Y.; *J. Phys. Chem. B* **2006,** *110*, 15666.

Received: June 12, 2007
Web Release Date: July 31, 2008